Model-Based Thermal History Control

Suhail S. Saquib and William T. Vetterling
Polaroid Corporation
Waltham, Massachusetts

Abstract

Heat diffusion within a thermal printhead leads to interactions between printed image pixels over both long and short distances, and results in a sharpness degradation and a distortion of the tone-scale. The loss in image quality is severe, especially if the thermal printhead is efficient and is printing at high speed. We present a novel multi-resolution thermal history control algorithm that delivers a requested print density via a physical model of heat propagation and an empirical model of the media response. The algorithm comprises three recursions, two in scale and one in time. This multi-scale recursive formulation leads to a computationally efficient real-time implementation. Experimental results demonstrate: 1) significantly improved SQF, 2) accurate dynamic and steady-state tone-scale reproduction and 3) equalization of leading, trailing and lateral edge sharpness.

Introduction

Thermal printers typically contain a printhead with a linear array of resistive heaters, and media that is thermally activated. The heaters can be independently turned on or off to adjust the printed density along a row of pixels. An image is produced by printing one line at a time as the printhead moves down the page.

Since the printing is enabled by heat, the printed pixel density is sensitive to ambient temperature. Furthermore, as printing proceeds, the printhead structure heats up, and also affects the printed density. Accurate control of the printing process therefore depends on a knowledge of the energy applied in the past. An algorithm that modifies the input energy so that the resulting print is independent of the ambient temperature and past printing is known as thermal history control (THC).[1,2]

Thermal history control is particularly important when the printhead is efficient or when fast printing speed is desired. The efficiency of a printhead is controlled by the thickness of an insulating glaze layer between the resistive heaters and a heat sink. Thicker glaze permits less heat loss to the heat-sink, and results in higher temperatures for the same applied energy, but it also makes the printer more sensitive to the previously printed lines because residual heat from those lines is not dissipated as quickly.

Fast printing also increases the sensitivity of printing to thermal history. In this case, a smaller line time allows insufficient time for the printhead to cool between the printing of one line and the next. This also affects the ability to print low densities immediately after high den-sities (trailing edges) or high densities immediately after low densities (leading edges). When the printhead is mov-ing quickly over the medium, even a small thermal time-constant translates into a large distance on the medium, and results in noticeable blurring of printed edges.

Model for Thermal History Control

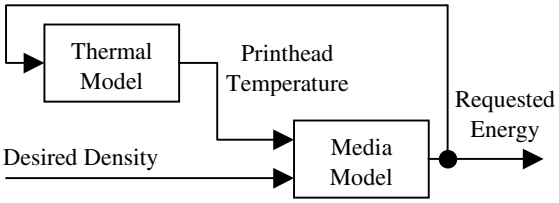

Figure 1. Block diagram of THC model

Figure 1 illustrates the components of our THC algorithm. The thermal model predicts the temperature rise of the printhead elements over time, given the applied energy, while the media model determines the energy needed to achieve a desired printed density.

Thermal Model

A typical thermal printhead has a layered construction comprising different materials such as glaze, ceramic and aluminum (See Fig. 2).

The temperature of the aluminum heat-sink can be assumed to be approximately constant during the printing of a single image due to its large thermal mass. A sensor is attached to the heat-sink to measure its temperature.

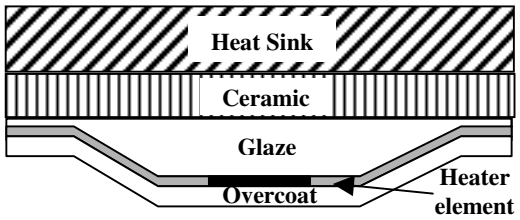

Figure 2. Schematic of a printhead showing the layered construction

The thermal model attempts to predict the temperature of the heater elements (pixels) based on the applied energy. Rather than modeling the pixel temperature directly, we divide the structure, with the heat sink on top and the pixels on the bottom, into layers and model the temperature differences between these layers. Each layer has an associated relative temperature with respect to the layer above it. The absolute temperature of a pixel is then obtained by summing the relative temperatures for all the layers, and adding the heat-sink temperature measured by the sensor.

Such a formulation has two distinct advantages that result in a very efficient algorithm: First, the relative temperature of each layer can be modeled by a simple recursion in time and space. Second, the layers that are further away from the heaters may be modeled at lower resolution (in both space and time) than layers that are closer to the heaters, giving rise to an efficient multi-resolution recursive computation.

Note that the model layers need not have a one-to-one correspondence with the physical layers of the printhead. Indeed, each physical layer in the head may be represented by multiple layers in the thermal model or vice versa.

Notation

Let d represent an image of density values to be printed, and E the input energy to the head. T_a and T will denote the absolute and relative temperature respectively. The superscript $^{(l)}$ denotes the layer number, and also the associated resolution of that layer, e.g. $T^{(l)}$. Layer $l=0$ corresponds to the finest resolution and layer $l=L-1$ to the coarsest resolution. The value $l=L$ is also used, and refers to the heat-sink, which has a single temperature value T_s obtained from the sensor attached to the heat-sink. Let n be the discrete time index and j the discrete space index, e.g., $T^{(l)}(n,j)$ denotes the relative temperature of spatial element j at time n in layer l. The number of time and spatial indices in each layer decreases with increasing l and are given as $N^{(l)}$ and $J^{(l)}$ respectively. I_l^m denotes the interpolation or decimation operator from layer l to layer m. Since the lowest-numbered layer has the highest resolution, and the highest-numbered layer has the lowest resolution, I_l^m is an interpolation operator when $l>m$ and it is a decimation operator when $l<m$.

Relative & Absolute Temperature

During printing, heat generated by the heater elements propagates to the heat-sink. Each layer in the model has a net loss of heat to the layer above it. This heat loss is proportional to the temperature gradient, and therefore to the relative temperature as defined above. Each layer is also receiving heat in proportion to the applied energy at the heater elements. The following time update formula therefore applies to the relative temperature of each layer

$$T^{(l)}(n,j) = T^{(l)}(n-1,j)\alpha_l + E^{(l)}(n-1,j)A_l,\ n=1,\ldots,N^{(l)}-1, \quad (1)$$

where α_l and A_l are layer parameters and $E^{(l)}$ is the applied energy at resolution l. Note that $E^{(0)}$ is the energy applied to the pixels whereas $E^{(l)}$ for $l>0$ is a lower resolution version of $E^{(0)}$ that can be recursively computed in scale as

$$E^{(l)} = I_{l-1}^{l} E^{(l)},\ \ l>0. \quad (2)$$

The algorithm for determining the energy to apply to the pixels, $E^{(0)}$, is dealt with in the "Media Model" section.

In addition to the upward heat flow, there is also heat flow in the lateral dimension within each layer. We account for this by computing a spatial heat diffusion on the relative temperatures following the time update of Eq. (1). The spatial update is given as

$$T^{(l)}(n,j) = (1-2k_l)T^{(l)}(n,j) + k_l(T^{(l)}(n,j-1) + T^{(l)}(n,j+1)), \quad j=1,\ldots,J^{(l)}-2, \quad (3)$$

where k_l is a lateral diffusion layer parameter. The absolute temperature of the pixels can finally be computed by propagating the absolute temperatures downwards through the layers starting from the temperature measured by the temperature sensor. This results in a recursive computation in scale given as

$$T_a^{(l)}(n,j) = \begin{cases} T_s(n), & l=L, \\ \left(I_{l+1}^{l} T_a^{(l+1)}\right)(n,j) + T^{(l)}(n,j), & l=L-1,\ldots,0. \end{cases} \quad (4)$$

Note that $T_s(n)$ does not have a spatial index since there is only a single value that is read from the temperature sensor.

Media Model

The role of the media model is to determine the energy required to achieve a desired density, given the absolute temperature of the heater element. In general, this will be a two-dimensional function given as

$$E^{(0)}(n,j) = f(T_a^{(0)}(n,j), d(n,j)). \quad (5)$$

However, estimation of the function $f(\cdot)$ directly from measured data is difficult since the number of parameters required to represent the function is large. Furthermore, computation of the energy from Eq. (5) would represent a significant computational burden. This problem is addressed by approximating energy Eq. (5) with two terms of a Taylor series expansion, as follows

$$E^{(0)}(n,j) = G\left(d(n,j)\right) + S\left(d(n,j)\right)T_a^{(0)}(n,j). \quad (6)$$

Here, $G(\cdot)$ and $S(\cdot)$ are one-dimensional functions that give the base energy and its sensitivity to temperature, respectively, at any given density.

Thermal History Control Algorithm

The THC model formulated in the previous section requires feedback as shown in Fig. 1. The energy to be applied to a pixel is determined from the media model using the current temperature of the pixel. This energy is then fed back to the thermal model to determine the temperature of the pixel at the next time instant. The inter-dependency of equations is clearly seen in Eqs. (1)-(6). Computations must be

Global $\bar{E}^{(l)} = 0,\ \bar{T}^{(l)} = 0,\ \bar{T}_a^{(l)} = T_s(0),\ n = 0$

While(n< $N^{(0)}$) ComputeEnergy (*L-1*) // process image

ComputeEnergy(*l*) {
// Update $T^{(l)}$ using Eqs. and
if ($l \neq 0$) {
$\overline{incr}^{(l)} = \left(I_{l+1}^{l}\bar{T}_a^{(l+1)} + \bar{T}^{(l)} - \bar{T}_a^{(l)}\right) \Big/ D_{l,l-1}$
$\bar{E}^{(l)} = 0$
repeat $D_{l,l-1}$ times {
$\bar{T}_a^{(l)} = \bar{T}_a^{(l)} + \overline{incr}^{(l)}$ (Eq. (4))
ComputeEnergy(*l-1*)
$\bar{E}^{(l)} = \bar{E}^{(l)} + I_{l-1}^{l}\bar{E}^{(l-1)} \Big/ D_{l,l-1}$ (Eq.)
if ($n \geq N^{(0)}$) return
}
} else {
$\bar{T}_a^{(0)} = I_1^0\bar{T}_a^{(1)} + \bar{T}^{(0)}$
Compute $\bar{E}^{(0)}$ using (Eq.)
n=n+1
}
}

Figure 3.Pseudo code for the THC algorithm

performed in a certain order to ensure the availability of all variables contributing to the quantity being computed. This section presents pseudo code that achieves this via a recursion in scale that is initiated at the coarsest resolution.

The recursion in scale applies both to the time and spatial dimensions of the image. However, as the calculation proceeds stepwise along the time dimension, interpolations and decimations are performed only on the spatial dimension. All of the two-dimensional variables used in the above equations, such as *T, E,* and T_a are consequently stored as one-dimensional variables that simply change in value from one time-step to the next. At any time step, the interpolation or decimation operators I_l^m used in the pseudo code operate only on the space dimension.

The interpolation of absolute temperature from scale *l* to *l-1* along the time dimension is handled in the following way: The array $\overline{incr}^{(l)}$ is used* to store the current increment of the absolute temperature of layer *l* per unit time-step in layer *l-1*. The time-interpolated value of the absolute temperature at the next time instant for the layer below is obtained by adding this increment to the current absolute temperature. The decimation in time for the energy of any layer *l>0* is obtained by accumulating the energies of the layer *l*-1 in the energy array $\bar{E}^{(l)}$. $D_{l,l-1}$ is used to denote the decimation factor between layers *l* and *l-1*. The pseudo code shown in Fig. 3 uses linear interpolation for operator I_l^m when *l>m* and simple averaging when *l<m*.

* Symbol names with overbars denote 1-D arrays. e.g. $\overline{incr}^{(l)}$, $\bar{E}^{(l)}$, $\bar{T}^{(l)}$ and $\bar{T}_a^{(l)}$ are all arrays of length $J^{(l)}$.

Parameter Estimation

To make use of this THC model, the parameters $\alpha_l, A_l, k_l, G(\cdot)$ and $S(\cdot)$ functions must be estimated. This is done by formulating a printer model that predicts the printed density when a known energy image is applied to the printer. In this case, the thermal model may be used as is, but the media model must be used in an inverse sense. That is, instead of determining the energy given the temperature and desired density, we need to determine the density given the temperature and applied energy. This is accomplished by finding the root d of non-linear Eq. , given $E^{(0)}$ and $T_a^{(0)}$, using a bisection method.[3] THC parameters are then obtained by minimizing the mean square error between the printer model predictions and measured density data.

A parametric representation of the functions $G(\cdot)$ and $S(\cdot)$ is desirable to facilitate their estimation. The function $G(\cdot)$ maps density to energy, which is inverse of the printer system response function $\Gamma(\cdot)$ that maps input energy to output density. Since typical $\Gamma(\cdot)$ functions of thermal printers are "S" shaped, we choose the following parametric representation

$$d = \Gamma(E) = \frac{d_m}{1+\exp(-4\sigma\left(a(E-E_c)^3 + b(E-E_c)^2 + (E-E_c)\right)}, \quad (7)$$

where d_m represents the maximum density the printer is capable of producing and σ is the slope of the function at the point of symmetry, E_c, when $a = b = 0$. Non-zero values of a and b distort the energy axis yielding an asymmetrical function that permits a better fit to the data. We choose $G(d) = \Gamma^{-1}(d)$. The shape of the sensitivity function $S(\cdot)$ is much more variable and depends on the characteristics of the thermal media. For generality, $S(\cdot)$ is modeled by a polynomial whose order is typically chosen to be 3 or 4.

Results

The THC algorithm described has been very successful in correcting for thermal effects for a number of different thermal media, including D2T2,[4] a proprietary thermal transfer medium known as OPAL[5] and a direct thermal medium. In this Section, we present results for the OPAL medium.

The OPAL system consists of a donor ribbon coated with a thermally sensitive dye layer, and a porous receiver. The dye layer is a self-supporting dye glass that allows a very high writing speed. OPAL printers, in fact, are capable of printing photographic quality 4 x 6 images in 2 seconds each. Efficient thermal printing at this speed requires accurate thermal history compensation, for reasons stated above.

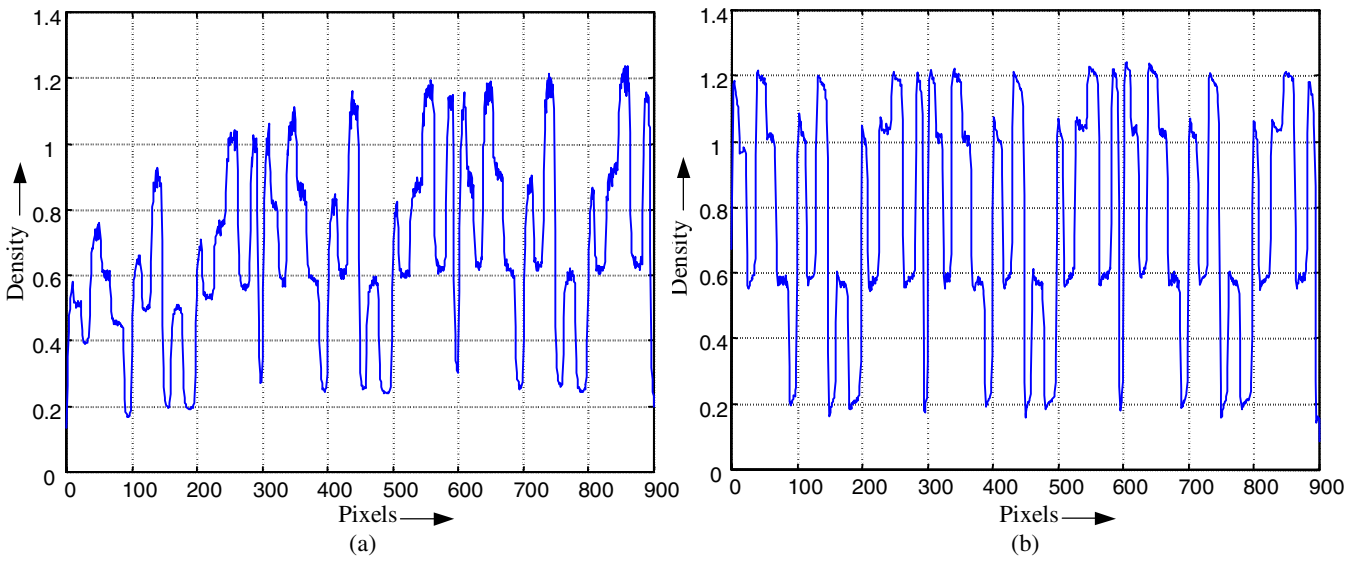

Figure 4. The density response of an OPAL thermal printer with (a) no THC and (b) with THC. There were four unique densities in the target 0.2, 0.6, 1.0 and 1.2. These desities are accurately reproduced in (b) but drift significantly in (a).

Figure 4 shows the results of applying the THC algorithm to an OPAL thermal printer, printing at 3 in/sec with a resolution of 266 dpi in the down-web direction. The test image was made up of horizontal bars. The density of each bar was randomly chosen from a set of 4 unique densities. The printed image was scanned and averaged in the horizontal direction to produce a one-dimensional density profile of the test image in the print direction. Figure 3(a) shows the density profile when no THC was performed. The plot shows that as the printer heats up, the printed density also increases rendering the requested 4 unique densities incorrectly. Furthermore, the edges of the bars are smooth giving an overall fuzzy appearance to the printed image. Fig. 3(b) shows that both of these problems are corrected when we process the image with THC. The 4 unique densities are reproduced on the print with high fidelity and the bar edges have distinct transitions giving the print a very sharp appearance.

To test the reproduction of edges with THC, we created a target that had edges of various contrasts and orientations. A low density region followed by a high density region in the print direction creates a leading edge (low-high transition) while a high-low transition creates a trailing edge. Fig. 5 plots the edge sharpness in the test target in terms of its SQF.[6] These results, and equivalent measurements for lateral edges are tabulated in Table 1.

Table 1. Sharpness (SQF) with and without thermal history control

	Without THC	With THC
Leading Edge	55	84
Trailing Edge	60	85
Lateral Edge	73	85

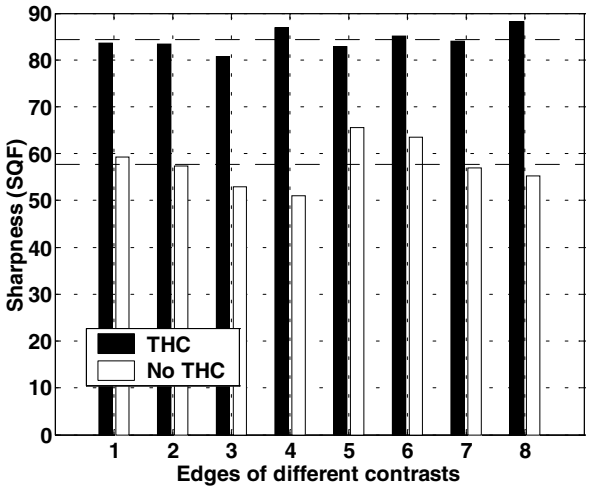

Figure 5. The sharpness of edges with different contrasts is plotted with and without THC. Edges 1-4 are leading edges and edges 5-8 are trailing edges.

The figure shows that without THC the sharpness of the edges depends on the contrast, and the average SQF is only about 57, resulting in a "blurry" appearance. On the other hand, with THC the edge sharpness is almost independent of contrast and edge type. The average SQF produced with THC is about 84, giving a sharp image.

Conclusion

We have described an efficient algorithm for compensating the thermal interactions that compromise the sharpness and accuracy of images produced by a thermal printer. Using a multi-resolution recursive algorithm, the corrections may be made in real-time, and they result in substantial improvements in the sharpness, tone-scale accuracy and reproducibility of images

References

1. N. Katsuma and H. Enomoto, U. S. Patent 5,800,075, "Data Processing Method for Eliminating Influence of Heat Accumulating in Thermal Head", (1998).
2. A. Someya, U. S. Patent 5,006,866, "Thermal Printing Apparatus Responsive to Estimated Stored Heat of the Heating Element", (1991).
3. W. Press et al., *Numerical Recipes in C: The Art of Scientific Computing*, Cambridge University Press, Cambridge, UK (1992).
4. R. A. Hann and N. C. Beck, "Dye Diffusion Thermal Transfer (D2T2) Color Printing," *J. Imaging Tech.*, **16**, 238-241, (1990).
5. S. J. Telfer and W. T. Vetterling, "Self Supporting, Two-Phase Binderless Film for Rapid Thermal-Transfer Printing," Proc. of 224th Am. Chem. Soc. Meeting, Boston, Aug 18-22, 2002.
6. E. M. Granger and K. N. Cupery, *J. Imaging Sci. and Tech.*, **42**, 112 (1998).

Biography

Suhail S. Saquib received his B.Tech. degree in Electronics and Electrical Communication Engineering from Indian Institute of Technology, Kharagpur, India, in 1991. He received his M.S. and Ph.D. degrees from Purdue University in 1992 and 1997 respectively. During the summer of 1996, he worked at Los Alamos National Laboratories in the area of medical optical tomography. Since 1997 he has been a member of the Image Science Lab. at Polaroid Corporation. His interests include ill-posed inverse problems, model-based image reconstruc-tion techniques, numerical methods, tomography, and pattern recognition.

William Vetterling received his B.A. degree in Physics from Amherst College in 1970, and a Ph.D. in Solid State Physics from Harvard University in 1976. He taught Physics at Harvard until 1984, when he joined the Microelectronics Division of Polaroid Corp. His work has focused on the design of electronic imaging and printing systems, and he is currently Distinguished Scientist at Polaroid's Image Science Laboratory. He is a member of the American Physical Society, the IEEE, the IS&T and the SPIE.